HHS Public Access

Author manuscript

Cell Rep. Author manuscript; available in PMC 2016 June 23.

Published in final edited form as:

Cell Rep. 2015 June 23; 11(11): 1797–1808. doi:10.1016/j.celrep.2015.05.025.

Hepatic SirT1-Dependent Gain-of-Function of Stearoyl-CoA Desaturase-1 Conveys Dysmetabolic and Tumor Progression Functions

Li Qiang[1,5], **Ning Kon**[2,5], **Wenhui Zhao**[2], **Le Jiang**[2], **Colette M. Knight**[3], **Carrie Welch**[1], **Utpal Pajvani**[1], **Wei Gu**[2,4], and **Domenico Accili**[1,4]

Wei Gu: wg8@columbia.edu; Domenico Accili: da230@cumc.columbia.edu

[1]Naomi Berrie Diabetes Center and Department of Medicine

[2]Institute for Cancer Genetics and Department of Pathology, College of Physicians and Surgeons, Columbia University New York, NY 10032

[3]Department of Medicine, Diabetes Research Center, Albert Einstein College of Medicine, Bronx, NY 10461

SUMMARY

Obesity is associated with higher incidence of cancer but the predisposing mechanisms remain poorly understood. The NAD^+–dependent deacetylase SirT1 orchestrates metabolism, cellular survival, and growth. To date, there is no unifying mechanism to explain the metabolic and tumor-related effects of SirT1. In this work, we demonstrate that genetic ablation of the endogenous inhibitor of SirT1, *Deleted-in-Breast-Cancer-1* (*Dbc1*), unexpectedly results in obesity and insulin-resistance. *Dbc1* deficiency promoted SirT1-dependent gain-of-function of stearoyl-coenzyme A desaturase 1 (Scd1), increasing plasma and tissue levels of unsaturated fatty acids. The metabolic abnormalities in $Dbc1^{-/-}$ mice were reversed by ablation of hepatic SirT1 or by inhibition of Scd1 activity. Furthermore, loss of *Dbc1* impaired master tumor suppressor p53 activation and treatment of Scd1 inhibitor extended survival of tumorigenic $TP53^{-/-}$ mice by decreasing tumor-related death. Together, our findings illustrate a shared mechanism of obesity and tumor progression through hepatic SirT1 gain-of-function in a metabolic control step, with potential therapeutic implications.

Correspondence to: Wei Gu, wg8@columbia.edu; Domenico Accili, da230@cumc.columbia.edu.

[4]Co-senior author

[5]Co-first author

Author Contributions

L.Q. and N. K. designed, executed, and analyzed the experiments and wrote the manuscript. W. Z. and L. J. executed the ChIP analysis. C.M.K. executed clamp studies. C. W. analyzed atherosclerosis lesion size. U. P. analyzed the experiments. D.A. and W. G. designed and reviewed the experiments and wrote the manuscript. D.A. and W. G. designed and supervised experiments, wrote the manuscript, and oversaw research.

INTRODUCTION

The rising prevalence of obesity and overweight is expected to result in ~500,000 excess deaths from cancer by 2030 (Wang et al., 2011). Although a well-documented association exists between obesity and cancer, especially among patients at the highest extremes of body mass index distribution, it remains unclear whether the association of obesity with cancer portends shared cellular and biochemical mechanisms, or simply reflects prevalent environmental, behavioral, and genotoxic susceptibilities (Wang et al., 2011). At the cellular level, different signaling pathways, such as insulin/IGF, AKT and mTORC, share metabolic and oncogenic functions (Gallagher and LeRoith, 2013).

The NAD^+–dependent, class III histone deacetylase (HDAC) SirT1 is another important control node of metabolism and oncogenesis (Chang and Guarente, 2014). SirT1 deacetylates proteins with complex roles in metabolism, inflammation, aging, cancer cell proliferation, and apoptosis. For example, it regulates hepatic gluconeogenesis through FOXO1 (Frescas et al., 2005; Qiang et al., 2010), white fat remodeling through peroxisome proliferator-activated receptor gamma (PPARγ) (Qiang et al., 2012), mitochondrial biogenesis through peroxisome proliferator-activated receptor gamma coactivator 1-alpha (PGC1α) (Rodgers et al., 2005), cholesterol metabolism through liver X receptor (LXR) (Li et al., 2007b), and other metabolic processes. The overall metabolic effects of moderate SirT1 gain-of-function are to lower energy efficiency and protect against obesity-induced diabetes (Banks et al., 2008; Pfluger et al., 2008). With regard to cancer biology, SirT1 deacetylates p53 to dampen its tumor-suppressor function (Luo et al., 2001), and may also regulate retinoblastoma protein (Rb) (Wong and Weber, 2007), E2F1 (Wang et al., 2006), c-Myc (Mao et al., 2011) and Poly (ADP-ribose) polymerase 1 (PARP-1) (Rajamohan et al., 2009). Nevertheless, to date, there is no unifying mechanism to explain the metabolic and tumor-related effects of SirT1.

Deleted-in-Breast-Cancer-1 (Dbc1) is an endogenous inhibitor of SirT1 (Kim et al., 2008; Zhao et al., 2008) that is expected to regulate the latter's ability to acetylate p53, thus promoting cell cycle arrest, apoptosis and senescence (Li et al., 2012). In support of this notion, it is found that regulation of SirT1 by Dbc1 is altered in various types of cancers (Hiraike et al., 2011; Kim et al., 2009; Sung et al., 2010), implicating a tumor suppressor-like function of Dbc1. However, there is no direct evidence that Dbc1 is a tumor suppressor. Similarly, there is evidence that Dbc1 deletion prevents diet-induced hepatosteatosis in mice, but the mechanism of this effect is not known (Escande et al., 2010). Besides its function to inhibit SirT1, Dbc1 also regulates other chromatin remodeling enzymes, such as HDAC3 and SUV39H1, as well as transcription factors, including androgen receptor, estrogen receptor α and β, RARα, Rev-erbα, MYC, and BRCA1, either as an activator or repressor (Joshi et al., 2013). Interestingly, the interaction between Dbc1 and SirT1 is regulated during diet-induced obesity (Escande et al., 2010; Escande et al., 2015), raising the question of whether Dbc1 participates in the etiology of the metabolic syndrome.

In this work, we set out to investigate the metabolic functions of Dbc1 in association with its growth regulatory functions, and asked whether these functions are mediated by SirT1. In studies of *Dbc1*-deficient mice, we found insulin resistance with increased body fat content

and impaired activation of tumor suppressor p53. These changes were associated with increased SirT1-dependent expression of *Scd1*, and altered tissue and plasma levels of unsaturated fatty acids. When the increase of Scd1 was reversed by pharmacological inhibition, metabolic and tumor-progression phenotypes were reversed, consistent with the possibility that Scd1 mediates both metabolic and oncogenic branches of the SirT1 pathway, and providing a potential mechanism for the baffling increase of cancer in metabolic diseases.

RESULTS

Dbc1$^{-/-}$ Mice Develop Insulin Resistance and Increased Body Fat

Given the pivotal functions of SirT1 in the pathophysiology of metabolic disorders, we investigated whether its native inhibitor Dbc1 also plays a role in metabolism. To this end, we generated *Dbc1* knockout mice (Figures S1A–D). The knockouts were born in Mendelian ratios and showed normal features, growth rates, and reproductive behavior. Since ablation of *Dbc1* increases SirT1 activity (Escande et al., 2010; Escande et al., 2015), we expected that *Dbc1*$^{-/-}$ mice would be more insulin-sensitive and protected against obesity-induced diabetes (Banks et al., 2008; Pfluger et al., 2008). Surprisingly, *Dbc1*$^{-/-}$ mice developed impaired tolerance to an intraperitoneal glucose load as early as 16 weeks after birth and remained glucose intolerant throughout life (Figure 1A and Figures S2A–S2E). Circulating insulin levels also rose, consistent with systemic insulin resistance (Figure 1B). These changes were not accompanied by changes in body weight (Figure 1C), but rather by an increase in body fat content beginning at puberty (Figure 1D and Figure S2F). To explain these changes, we studied energy balance using indirect calorimetry. *Dbc1*$^{-/-}$ mice had similar respiratory exchange ratios (RER) as littermate controls (Figure S3A), but decreased locomotor activity (Figure 1E) and O_2 consumption (Figure 1F), as well as energy expenditure (Figure S3B). *SirT1* transgenics have similar decreases (Banks et al., 2008), supporting a SirT1 gain-of-function in *Dbc1* knockouts. But unlike *SirT1* transgenics, *Dbc1*$^{-/-}$ had similar food intake to control littermates (Figure S3C).

Metabolic Abnormalities in *Dbc1*$^{-/-}$ Are Exacerbated by High Fat Diet

Overexpression of SirT1 protects mice from obesity-induced insulin resistance, but not obesity (Banks et al., 2008). In contrast, when fed an obesogenic high-fat diet, *Dbc1*$^{-/-}$ mice displayed increased body weight (Figure 2A) and body fat content (Figure 2B), further impairment of glucose tolerance (Figure 2C), and higher insulin levels than wild-type controls (Figure 2D), without changes to glucose levels (not shown). These findings, consistent with impaired insulin sensitivity, were borne out by insulin tolerance tests (Figure 2E). Given the role of SirT1 in regulating hepatic glucose production (Banks et al., 2008), we tested whether glucose intolerance in *Dbc1*$^{-/-}$ was due to hepatic insulin resistance. During hyperinsulinemic-euglycemic clamps, *Dbc1*$^{-/-}$ mice displayed similar rates of glucose infusion (GIR) and disposal (Rd) (not shown), but increased basal hepatic glucose production (Figure 2F). In agreement with these findings, we found that glucose production by primary hepatocytes isolated from *Dbc1*$^{-/-}$ mice was also increased by ~ 50%, consistent with a cell-autonomous effect (Figure 2G). In summary, *Dbc1*$^{-/-}$ mice are prone to insulin resistance and diet-induced obesity.

Increased Scd1 in *Dbc1*$^{-/-}$ Mice

Dbc1$^{-/-}$ mice have been reported to have increased browning of white adipose tissue (WAT), a process against the development of obesity (Qiang et al., 2012). Thus, the normal body weight in *Dbc1*$^{-/-}$ (Figure 1C) could represent a compensatory mechanism from enhanced thermogenesis at ambient temperature. As expected, knockouts gained more body weight than controls at thermo neutrality (32–33°C) (data not shown), further demonstrating a predisposition to obesity in *Dbc1*$^{-/-}$. We then hypothesized that their metabolic alterations affect lipid homeostasis. Therefore, we surveyed expression of genes required for lipid synthesis and turnover in livers of *Dbc1*$^{-/-}$ mice. Strikingly, whereas most regulators of lipid transport and synthesis–including *Srebf1, Fasn, Acc2, Dgat2, Pparγ,* and *Cd36*–were expressed at or near wild-type levels, expression of *Scd1*, the rate-limiting enzyme in fatty acid (FA) desaturation, increased threefold above controls (Figure 3A). Elevation of *Scd1* also occurred in livers of HFD-fed *Dbc1*$^{-/-}$ mice.

In this instance, it was accompanied by smaller increases in other lipogenic genes (Figure 3B). Scd1 protein levels mirrored the mRNA findings (Figures 3C and 3D). To determine whether the increase in Scd1 was secondary to obesity and/or hepatocyte cell-autonomous, we assessed Scd1 activity in primary hepatocytes isolated from young *Dbc1*$^{-/-}$ mice prior to the onset of obesity and insulin resistance. To this end, we measured the ratio of the Scd1 product, stearoyl-CoA (C18:1), to its substrate oleoyl-CoA (C18:0). We found that the C18:1/C18:0 ratio increased threefold in *Dbc1*$^{-/-}$ *vs*. wild-type hepatocytes (Figure 3E), parallel to the levels of Scd1 (Figure 3F). These data indicate that *Scd1* activation is a cell-autonomous effect of Dbc1 loss that precedes the onset of obesity in *Dbc1* knockouts.

Paradoxical Protection from Atherosclerosis by Deletion of *Dbc1*

Scd1 deficiency has a paradoxical effect to increase atherosclerosis even though these mice are protected from obesity and insulin resistance (Brown et al., 2008; MacDonald et al., 2009). We then hypothesized that, if the metabolic phenotypes of *Dbc1*$^{-/-}$ are mediated by Scd1, *Dbc1* knockouts should also be protected from atherosclerosis. In *Dbc1*$^{-/-}$*:Ldlr*$^{-/-}$ double knockouts fed a western-type diet (WTD), we confirmed the increase of Scd1 (Figures S4A and S4B) as well as a constellation of atherogenic findings, including increased body weight, hepatosteatosis, dyslipidemia, and insulin resistance (Table S1). However, atherosclerotic lesion size was decreased in *Dbc1*$^{-/-}$ *:Ldlr*$^{-/-}$ mice, consistent with a protective function of Scd1 against plaque formation (Erbay et al., 2009), and in line with the anti-atherogenic function of *Dbc1* deficiency in *ApoE*$^{-/-}$ mice (Escande et al., 2015). These data buttress the conclusion that Scd1 activation is mechanistically responsible for the phenotype of *Dbc1*$^{-/-}$ mice. Indeed, the metabolic sub-phenotypes of *Dbc1*$^{-/-}$ mice are opposite to those found in *Scd1*-deficient mice (Table S2).

Dbc1 Deletion Further Impairs Metabolic Control in *ob/ob* Mice

Scd1 ablation reduces body weight in *leptin*-deficient *ob/ob* mice (Cohen et al., 2002). Thus, we asked whether deletion of *Dbc1* affects obesity in *ob/ob* mice. As expected, we saw increased body weight, fat content, decreased lean mass, and impaired glucose tolerance in *Dbc1*$^{-/-}$*:ob/ob* mice (Figures S4C–S4E). The additive effects of the *Dbc1* and *ob* mutations

indirectly rule out impaired leptin signaling as a primary cause of obesity and insulin resistance in *Dbc1*$^{-/-}$ mice.

Inhibition of Scd1 Restores Metabolic Homeostasis in *Dbc1*$^{-/-}$ Mice

To test whether the metabolic abnormalities of *Dbc1*$^{-/-}$ mice were mediated by Scd1, we treated HFD-fed mice with the Scd1 inhibitor, A939572 (Flowers et al., 2011; Paton and Ntambi, 2010). Treatment with low doses of inhibitor affected weight gain in control mice as expected, but more importantly, normalized body weight gain (Figure 4A) and abnormal body composition in the knockouts (Figure 4B and 4C). Consistent with our findings in primary hepatocytes (Figure 3F), monounsaturated FA content (MUFA, C18:1) increased in livers of *Dbc1*$^{-/-}$ mice and were normalized by treatment with the inhibitor (Figure 4D). There was no effect on hepatic lipid content (Figures S5A–S5C). Furthermore, glucose intolerance in *Dbc1*$^{-/-}$ mice was also improved by low-dose Scd1 inhibitor treatment (5 vs. 10–100 mg/kg/day) (Figure 4E). These data support the conclusion that the metabolic effects of *Dbc1* ablation require Scd1 gain-of-function.

Metabolic Abnormalities in *Dbc1*$^{-/-}$ Mice Are SirT1-Dependent

Next we asked whether the metabolic functions of Dbc1 are mediated through SirT1. To this end, and given the lethality associated with complete SirT1 deletion, we generated 1 (Figures S6A and S6B), *L-SirT1:Dbc1*$^{-/-}$ mice showed normal body weight (Figure S6C), fat content (Figure 5B), and glucose tolerance (Figure 5C). In fact, obesity and glucose intolerance in young *Dbc1*$^{-/-}$ mice were completely reversed by hepatic *SirT1* deletion (Figures S6D and S6E). When fed HFD, *L-SirT1:Dbc1*$^{-/-}$ mice gained less weight than controls (Figure 5E), and showed no increase in body fat (Figure 5F). More importantly, *Sirt1* ablation prevented the increase of *Scd1* in livers of *L-SirT1:Dbc1*$^{-/-}$ *mice* (Figure 5D). Taken together, the metabolic abnormalities in *Dbc1*$^{-/-}$ mice were offset by blocking SirT1-dependent up-regulation of Scd1 in the liver.

Scd1 Is Regulated by Dbc1 and SirT1

To understand the biochemical basis of the interaction among SirT1, Dbc1, and Scd1, we examined whether SirT1 and Dbc1 regulate activity of a minimal *Scd1* promoter encompassing −1537/+155 (Chu et al., 2006). Wild-type SirT1, but not its catalytically inactive mutant (H363Y), stimulated *Scd1* promoter activity, while Dbc1 repressed it (Figure 6A). Chemical inhibition of SirT1 repressed *Scd1* promoter activity, without affecting the related *Fasn* promoter (Figure 6B). Deletion mapping localized the Dbc1/SirT1 interaction site between bp −981 and −589 (Figure 6C). Chromatin immunoprecipitation assays further confirmed binding of Dbc1 to *Scd1* promoter between bp-807 to −428 (Figure 6D). Moreover, transient knockdown of *DBC1* increased SCD1 levels in human non-small cell lung cancer cells (Figure 6E), indicating that Dbc1 is a conserved negative regulator of *Scd1* in normal and carcinoma cells. Collectively, these data suggest that the deacetylase activity of SirT1 increases Scd1 expression, and that Dbc1 inhibits Scd1 by blocking SirT1.

Impaired p53 Activation in *Dbc1*$^{-/-}$ Mice

Next, we investigated the tumor-promoting properties of Dbc1. As predicted, *Dbc1* ablation reduced p53 acetylation and activation of its target genes *p21* and *puma* in embryonic fibroblasts (MEFs), following doxorubicin-induced DNA damage (Figures S7A–S7B). We then asked whether Dbc1 is a *de facto* tumor suppressor. Ionizing radiation induces p53, resulting in apoptosis, as indicated by the presence of cleaved Caspase-3 in thymus and spleen of irradiated wild-type animals (Figures 7A and 7B). Consistent with the findings in MEFs, *Dbc1*$^{-/-}$ mice showed a blunted p53 response and reduced Caspase-3 cleavage (Figure 7B). Based on the reduced p53 activation by DNA damage, we expected increased tumorigenesis in *Dbc1*$^{-/-}$ mice. But to our surprise, spontaneous tumors arose in aging *Dbc1*$^{-/-}$ mice at the same rate as in wild-type controls (not shown). Thus, *Dbc1* deletion is not oncogenic *per se*, but is expected to accelerate cancer progression owing to impaired p53 activation.

Scd1 Inhibition Prevents Cancer Progression in *TP53*$^{-/-}$ Mice

Similar metabolic abnormalities to those observed in *Dbc1* knockouts are associated with increased risk of cancer (Gallagher and LeRoith, 2013). Mice deficient in *p53* (*TP53*$^{-/-}$) develop spontaneous tumors and die by 6 months of age (Jacks et al., 1994). Interestingly, lack of *p53* in primary hepatocytes increased levels of Scd1 and MUFAs (Figures 7C and 7D). Therefore, we investigated whether the metabolic alterations in *Dbc1*$^{-/-}$ mice affected cancer susceptibility in an Scd1-dependent manner. Although SCD1 inhibitor has been shown to induce apoptosis in cultured cancer cells (Hess et al., 2010), and decrease tumor growth in a human gastric xenograft model at high doses (100mg/kg/BID) (Roongta et al., 2011), its anti-tumor function has never been tested *in vivo*. As a critical test of our hypothesis, we fed *TP53*$^{-/-}$ mice HFD and treated them with the Scd1 inhibitor at physiological dose (5mg/kg/day). Inhibitor-treated mice mimicked aspects of *Scd1*-deficient mice, including fur loss, eyelid closure, and body weight reduction (Miyazaki et al., 2001; Ntambi et al., 2002). Importantly, we observed a substantial reduction of tumor-related death and a 28% increase of median lifespan among inhibitor-treated mice, compared to untreated controls (Figure 7E).

DISCUSSION

Here we report SirT1-dependent elevation of Scd1 accounts for obesity and insulin resistance in *Dbc1*$^{-/-}$ mice under multiple genetic and dietary manipulations. Loss of Dbc1 enhanced SirT1 activity, consistent with previous studies in *Dbc1* knockout mice (Escande et al., 2010; Escande et al., 2015).

It is surprising that the gain-of–function of SirT1 associated with *Dbc1* ablation caused obesity and insulin resistance, unlike the gain-of-function caused by *SirT1* overexpression in transgenic mice (Banks et al., 2008; Pfluger et al., 2008). In the latter models, SirT1 is overexpressed at levels about twofold higher than endogenous, and is still under control by Dbc1, whereas in *Dbc1*$^{-/-}$ mice, SirT1 is constitutively active. This provides a potential explanation for the fact that Scd1 is increased in *Dbc1*$^{-/-}$, but not in *SirT1* transgenic mice (Qiang et al., 2011). In support of this notion, increased *Scd1* expression was observed in β

cells with 12- to 18-fold overexpression of *Sirt1* (Moynihan et al., 2005; Ramsey et al., 2008). The increase of *Scd1* by unchecked SirT1 activation is likely responsible for the unexpected obesity and insulin resistance of *Dbc1*$^{-/-}$ mice.

Several transcriptional factors, including SREBP-1c, LXRα and PPARs, activate *Scd1* (Chu et al., 2006; Paton and Ntambi, 2009). However, to our knowledge no *Scd1* repressors were known thus far. Our mapping data have identified a region in the promoter through which Dbc1 represses *Scd1*. The consensus binding sites for C/EBP, NF-Y/NF-1, SRE, Sp1 in the mouse *Scd1* promoter are conserved in the human *SCD1* promoter (Bene et al., 2001). Notably, we also saw regulation of SCD1 by *DBC1* knockdown in human cancer cells (Figure 6E and data not shown). We don't know whether the repression is direct or indirect, but it's unlikely to be mediated by Srebp-1c, as it's not associated with increases of other Srebp-1c targets, such as *Fasn*. Moreover, expression patterns of *Scd1* and *Srebp-1c* are distinct in *Dbc1*$^{-/-}$ mice. Finally, *Scd1* repression by Dbc1 requires SirT1 deacetylase activity, suggesting that it involves deacetylation of transcriptional regulators.

Ablation of *Dbc1* is not oncogenic *per se*, but likely favors tumor progression by impairing p53 activation through unchecked SirT1 activity. The function of SirT1 in cancer is context-dependent (Deng, 2009). SirT1 haploinsufficiency promotes spontaneous tumor development in *TP53*$^{+/-}$ mice, while overexpression of SirT1 in lymphocyte progenitors reduces the incidence of thymic lymphomas in *TP53*$^{+/-}$ mice post γ-irradiation, consistent with a tumor-suppressor function of SirT1. On the other hand, SirT1 is elevated in human leukemia, as well as prostate, colon, skin, and some hepatocellular cancers. Moreover, SirT1 levels correlate with malignancy of hepatocellular carcinoma. As SirT1 also impairs p53 acetylation and regulation of cell cycle, apoptosis and senescence (Li et al., 2012), a possible explanation of this apparent discrepancy is that SirT1 inhibits tumor initiation in normal cells, but facilitates progression in established tumors (Chang and Guarente, 2014; Chen et al., 2012). This view is consistent with the present observation that the tumor-promoting function of *Dbc1* ablation is associated with SirT1 activation, as well as with evidence of impaired regulation of SirT1 by Dbc1 in certain cancers (Hiraike et al., 2011; Kim et al., 2009; Sung et al., 2010).

Our findings suggest a mechanism whereby tumor progression genes can leverage a metabolic control step to promote cancer growth. Scd1 is the rate-limiting enzyme in generating mono-unsaturated FAs (MUFA). In addition to its critical role in lipid storage and obesity, unsaturated FA synthesis is required for membrane biogenesis, fluidity, and permeability, and hence by rapidly growing tumor cells. MUFAs are also involved in signal transduction to support cancer cell growth (Atilla-Gokcumen et al., 2014; Igal, 2011). Elevated Scd1 levels have been found in various human cancers with increased lipid desaturation (Fritz et al., 2010; Ide et al., 2013; Roongta et al., 2011; von Roemeling et al., 2013). These types of cancer are also commonly associated with obesity (Calle et al., 2003; Wang et al., 2011). Treatment with Scd1 inhibitor decreases proliferation and induces apoptosis in cancer cells (Hess et al., 2010; Roongta et al., 2011). Of particular interest is that theses anti-proliferative and pro-apoptotic effects of Scd1 inhibition are selective to tumor cells, but not to normal cells (von Roemeling et al., 2013). Therefore, the coordinated

regulation of *Scd1* by Dbc1 and SirT1 provides a heretofore-unknown mechanism for the predisposition to cancer associated with obesity.

The metabolic abnormalities in our *Dbc1*$^{-/-}$ mice are largely consistent with those in knockouts generated by genetrap methodology (Escande et al., 2010; Escande et al., 2015; Nin et al., 2014). In the latter model, female mice developed a “fit obese” phenotype, i.e., obesity with insulin sensitivity, and reduced adipocyte lipolysis (Escande et al., 2015). Neither in two previous reports (Escande et al., 2015; Nin et al., 2014), nor in our study are males protected from diet-induced insulin resistance, raising the possibility of sex-dimorphic actions of Dbc1. We did not observe protection from diet-induced steatosis on chow/HFD feeding (not shown) or through Scd1 inhibition (Figure S5), possibly due to different knockout strategies or experimental conditions. However, both *Dbc1* knockout models showed protection from atherosclerosis (Escande et al., 2015), in line with the anti-atherogenic functions of Scd1 (Erbay et al., 2009). The implication of the atherosclerosis studies is that targeting Dbc1/Scd1/MUFA may lessen the burden of atherosclerosis in obesity and type 2 diabetes.

In sum, we have uncovered a shared obesogenic and tumor-promoting mechanism resulting from gain-of-function of the fatty acid desaturase, Scd1, through derepression of SirT1. Our study, along with our previous report of pro-atherogenic effects of SirT1 (Qiang et al., 2011), adds to a body of work that invites caution in exploring the therapeutic applications of SirT1 activators (Alcain and Villalba, 2009; Chang and Guarente, 2014; Chen et al., 2008; Li et al., 2007b; Ng and Tang, 2013). In addition, our study contributes to mapping pathways of disease progression connecting obesity, insulin resistance, and cancer thus may pave the way to treating metabolic syndrome-related cancers.

EXPERIMENTAL PROCEDURES

Generation of *Dbc1* Knockout Mice

To construct *Dbc1* gene targeting vector, a fragment of *Dbc1* genomic DNA, containing 5.5 kb DNA 5’ of exon 1 and 1.8 kb 3’ of exon 1, was cloned by recombineering. Next, a promoter-less *EGFP* was inserted in exon 1 in frame next to the translation start codon (ATG) along with a neomycin resistance gene cassette allowing selection by G418. The targeted allele permits expression of *EGFP* controlled by endogenous *Dbc1* promoter (Figure S1A). The clones containing *EGFP-neo* cassette insertion through homologous recombination were screened by Southern blotting using EcoRV digested ES cell genomic DNA and an external 3’ probe, amplified using forward primer 5’-GTT GAT GAT ACA TTT TGA TCT CA-3’ and reverse primer 5’-AAG GTA GGA GCA GCA GAA ACC TG-3’ (Figure S1B). Targeted ES cell clones were injected into C57BL6/j blastocysts to derive chimeras, from which the targeted allele was transmitted successfully.

Animal Studies

Dbc1$^{-/-}$ mice were on 129/J x C57BL/6J background and *TP53*$^{-/-}$ mice on C57BL/6J background. *Lep*$^{ob/+}$ mice were from Jackson Laboratories (Bar Harbor, ME). *Ldlr*$^{-/-}$, α1-antitrypsin-cre transgenic (AT-Cre), and *Sirt1*$^{fllox/flox}$ mice (Li et al., 2007a) have been

described. Mice were housed at ambient temperature in a 12-hr light/dark cycle and fed *ad libitum* normal chow (PicoLab rodent diet 20) (LabDiet 5053), 60 kcal% high fat diet (Research Diet, D12492), or Western-type diet (TD88137, Harlan Teklad). Metabolic characterization was performed as described (Banks et al., 2008; Qiang et al., 2011; Qiang et al., 2012). All experiments were performed in male mice unless indicated. The Columbia University Animal Care and Utilization Committee approved all procedures.

Scd1 Inhibitor Treatment

For acute Scd1 inhibitor treatment, we injected A939572 (Biofine, Vancouver, Canada) intraperitoneally (i.p.) daily at a dose of 5 mg/kg starting on the same day as HFD. For chronic treatment in *TP53*$^{-/-}$ mice, the inhibitor was mixed with 60 kcal% HFD at a dose of 100mg/kg. Scd1 activities were determined by measuring saturated and unsaturated CoA concentrations at the Biomarkers Core Lab of the Irving Institute for Clinical and Translational at Columbia University.

Cell Culture and Scd1 Luciferase Reporter Assay

We transiently transfected HEK-293T cells (12-well) with 0.2μg *Luciferase* reporter plasmids and 0.02μg *Renilla* control plasmid, together with 0.2μg indicated SirT1 or Dbc1 plasmids using *Trans*IT-LT1 reagent (Mirus Bio). We then performed Dual-luciferase reporter assay by following the manufacturer's instructions (Promega, Madision, WI). Mouse *Scd1* promoter luciferase reporters (−1537/+155, −981/+155, −589/+89) are generously provided by Dr. James Ntambi (Chu et al., 2006). The *Fasn* luciferase reporter was used as a control. Glucose production in primary hepatocytes was performed as described (Pajvani et al., 2013).

Protein Analysis

Proteins were extracted into protein lysis buffer (50mM Tris, pH 7.4, 150mM NaCl, 10% glycerol, 2% NP-40, 1mM EDTA pH 8.0, 0.1% SDS, 0.5% NaDOC) supplemented with protease and phosphatase inhibitors. Antibodies used were: Dbc1 (Bethyl Laboratories, note: nonspecific signal at 135kD for freshly made working solution), p53 (CM5, Leica Microsystems), Puma (Sigma-Aldrich), SirT1 (Millipore), p21 and tubulin (Santa Cruz). Scd1, Fas, cleaved Caspase 3, Ac-p53, p-Akt (S473), p-Akt (T308), Akt and actin antibodies were purchased from Cell Signaling. HRP-conjugated secondary antibodies (GE Healthcare) were used for detecting ECL western blot signals.

Gene Expression Analysis

Total RNA was isolated with RNeasy Lipid Tissue kit (Qiagen) and 1μg RNA was subjected to cDNA synthesis by using High-capacity cDNA Reverse Transcription kit (Applied Biosystems). We performed Q-PCR with goTaq qPCR Master Mix (Promega) on CFX96 Real-Time PCR system (Bio-Rad). The relative gene expression levels were calculated by ΔΔCt method with *cyclophilin A* as the reference gene. Q-PCR primers were as listed (Qiang et al., 2011; Qiang et al., 2012).

ChIP Assay

We performed ChIP analysis of Dbc1 on Scd1 promoter by using ChIP assay kit following manufacturer's instructions (EMD Millipore). Anti-Dbc1 (Bethyl Laboratories) was used.

Histology

We used paraffin-embedded sections for Dbc1, p53 and Caspase-3 immunohistochemistry (all at 1:100 dilution) and frozen liver sections for Oil red-O staining.

Statistical Analysis

We performed unpaired 2-tail student's *t*-tests for single measurements and two-way ANOVA with Tukey post-hoc analysis where appropriate by using JMP software (SAS, NC) to evaluate statistical significance. $P < 0.05$ was considered as a significant change. All values are presented as means ± standard deviations (SD).

Supplementary Material

Refer to Web version on PubMed Central for supplementary material.

Acknowledgements

We thank T. Kolar and A. Flete for excellent technical assistance and members of Accili and Gu laboratories for critical discussions. We are grateful to Dr. J. Ntambi (University of Wisconsin at Madison) for *Scd1* reporter plasmids. This work was supported by National Institutes of Health grants DK97455 (LQ), CA172023 (WG), CA169246 (WG), CA085533 (WG), HL87123 (DA), DK63608 (Columbia University Diabetes Research Center), UL1TR000040 (National Center for Advancing Translational Sciences).

REFERENCES

Alcain FJ, Villalba JM. Sirtuin inhibitors. Expert opinion on therapeutic patents. 2009; 19:283–294. [PubMed: 19441904]

Atilla-Gokcumen GE, Muro E, Relat-Goberna J, Sasse S, Bedigian A, Coughlin ML, Garcia-Manyes S, Eggert US. Dividing cells regulate their lipid composition and localization. Cell. 2014; 156:428–439. [PubMed: 24462247]

Banks AS, Kon N, Knight C, Matsumoto M, Gutierrez-Juarez R, Rossetti L, Gu W, Accili D. SirT1 gain of function increases energy efficiency and prevents diabetes in mice. Cell Metab. 2008; 8:333–341. [PubMed: 18840364]

Bene H, Lasky D, Ntambi JM. Cloning and characterization of the human stearoyl-CoA desaturase gene promoter: transcriptional activation by sterol regulatory element binding protein and repression by polyunsaturated fatty acids and cholesterol. Biochem Biophys Res Commun. 2001; 284:1194–1198. [PubMed: 11414710]

Brown JM, Chung S, Sawyer JK, Degirolamo C, Alger HM, Nguyen T, Zhu X, Duong MN, Wibley AL, Shah R, et al. Inhibition of stearoyl-coenzyme A desaturase 1 dissociates insulin resistance and obesity from atherosclerosis. Circulation. 2008; 118:1467–1475. [PubMed: 18794388]

Calle EE, Rodriguez C, Walker-Thurmond K, Thun MJ. Overweight, obesity, and mortality from cancer in a prospectively studied cohort of U.S. adults. N Engl J Med. 2003; 348:1625–1638. [PubMed: 12711737]

Chang HC, Guarente L. SIRT1 and other sirtuins in metabolism. Trends in endocrinology and metabolism: TEM. 2014; 25:138–145. [PubMed: 24388149]

Chen D, Bruno J, Easlon E, Lin SJ, Cheng HL, Alt FW, Guarente L. Tissue-specific regulation of SIRT1 by calorie restriction. Genes Dev. 2008; 22:1753–1757. [PubMed: 18550784]

Chen HC, Jeng YM, Yuan RH, Hsu HC, Chen YL. SIRT1 promotes tumorigenesis and resistance to chemotherapy in hepatocellular carcinoma and its expression predicts poor prognosis. Ann Surg Oncol. 2012; 19:2011–2019. [PubMed: 22146883]

Chu K, Miyazaki M, Man WC, Ntambi JM. Stearoyl-coenzyme A desaturase 1 deficiency protects against hypertriglyceridemia and increases plasma high-density lipoprotein cholesterol induced by liver X receptor activation. Mol Cell Biol. 2006; 26:6786–6798. [PubMed: 16943421]

Cohen P, Miyazaki M, Socci ND, Hagge-Greenberg A, Liedtke W, Soukas AA, Sharma R, Hudgins LC, Ntambi JM, Friedman JM. Role for stearoyl-CoA desaturase-1 in leptin-mediated weight loss. Science. 2002; 297:240–243. [PubMed: 12114623]

Deng CX. SIRT1, is it a tumor promoter or tumor suppressor? International journal of biological sciences. 2009; 5:147–152. [PubMed: 19173036]

Erbay E, Babaev VR, Mayers JR, Makowski L, Charles KN, Snitow ME, Fazio S, Wiest MM, Watkins SM, Linton MF, et al. Reducing endoplasmic reticulum stress through a macrophage lipid chaperone alleviates atherosclerosis. Nat Med. 2009; 15:1383–1391. [PubMed: 19966778]

Escande C, Chini CC, Nin V, Dykhouse KM, Novak CM, Levine J, van Deursen J, Gores GJ, Chen J, Lou Z, et al. Deleted in breast cancer-1 regulates SIRT1 activity and contributes to high-fat diet-induced liver steatosis in mice. J Clin Invest. 2010; 120:545–558. [PubMed: 20071779]

Escande C, Nin V, Pirtskhalava T, Chini CC, Tchkonia T, Kirkland JL, Chini EN. Deleted in breast cancer 1 limits adipose tissue fat accumulation and plays a key role in the development of metabolic syndrome phenotype. Diabetes. 2015; 64:12–22. [PubMed: 25053585]

Flowers MT, Paton CM, O'Byrne SM, Schiesser K, Dawson JA, Blaner WS, Kendziorski C, Ntambi JM. Metabolic changes in skin caused by Scd1 deficiency: a focus on retinol metabolism. PLoS One. 2011; 6:e19734. [PubMed: 21573029]

Frescas D, Valenti L, Accili D. Nuclear trapping of the forkhead transcription factor FoxO1 via Sirt-dependent deacetylation promotes expression of glucogenetic genes. J Biol Chem. 2005; 280:20589–20595. [PubMed: 15788402]

Fritz V, Benfodda Z, Rodier G, Henriquet C, Iborra F, Avances C, Allory Y, de la Taille A, Culine S, Blancou H, et al. Abrogation of de novo lipogenesis by stearoyl-CoA desaturase 1 inhibition interferes with oncogenic signaling and blocks prostate cancer progression in mice. Molecular cancer therapeutics. 2010; 9:1740–1754. [PubMed: 20530718]

Gallagher EJ, LeRoith D. Epidemiology and molecular mechanisms tying obesity, diabetes, and the metabolic syndrome with cancer. Diabetes Care. 2013; 36(Suppl 2):S233–S239. [PubMed: 23882051]

Hess D, Chisholm JW, Igal RA. Inhibition of stearoylCoA desaturase activity blocks cell cycle progression and induces programmed cell death in lung cancer cells. PLoS One. 2010; 5:e11394. [PubMed: 20613975]

Hiraike H, Wada-Hiraike O, Nakagawa S, Saji S, Maeda D, Miyamoto Y, Sone K, Tanikawa M, Oda K, Nakagawa K, et al. Expression of DBC1 is associated with nuclear grade and HER2 expression in breast cancer. Experimental and therapeutic medicine. 2011; 2:1105–1109. [PubMed: 22977628]

Ide Y, Waki M, Hayasaka T, Nishio T, Morita Y, Tanaka H, Sasaki T, Koizumi K, Matsunuma R, Hosokawa Y, et al. Human breast cancer tissues contain abundant phosphatidylcholine(36ratio1) with high stearoyl-CoA desaturase-1 expression. PLoS One. 2013; 8:e61204. [PubMed: 23613812]

Igal RA. Roles of StearoylCoA Desaturase-1 in the Regulation of Cancer Cell Growth, Survival and Tumorigenesis. Cancers. 2011; 3:2462–2477. [PubMed: 24212819]

Jacks T, Remington L, Williams BO, Schmitt EM, Halachmi S, Bronson RT, Weinberg RA. Tumor spectrum analysis in p53-mutant mice. Curr Biol. 1994; 4:1–7. [PubMed: 7922305]

Joshi P, Quach OL, Giguere SS, Cristea IM. A Functional Proteomics Perspective of DBC1 as a Regulator of Transcription. Journal of proteomics & bioinformatics. 2013; (Suppl 2)

Kim JE, Chen J, Lou Z. DBC1 is a negative regulator of SIRT1. Nature. 2008; 451:583–586. [PubMed: 18235501]

Kim JE, Lou Z, Chen J. Interactions between DBC1 and SIRT 1 are deregulated in breast cancer cells. Cell Cycle. 2009; 8:3784–3785. [PubMed: 19855164]

Li H, Rajendran GK, Liu N, Ware C, Rubin BP, Gu Y. SirT1 modulates the estrogen-insulin-like growth factor-1 signaling for postnatal development of mammary gland in mice. Breast cancer research : BCR. 2007a; 9:R1. [PubMed: 17201918]

Li T, Kon N, Jiang L, Tan M, Ludwig T, Zhao Y, Baer R, Gu W. Tumor suppression in the absence of p53-mediated cell-cycle arrest, apoptosis, and senescence. Cell. 2012; 149:1269–1283. [PubMed: 22682249]

Li X, Zhang S, Blander G, Tse JG, Krieger M, Guarente L. SIRT1 deacetylates and positively regulates the nuclear receptor LXR. Mol Cell. 2007b; 28:91–106. [PubMed: 17936707]

Luo J, Nikolaev AY, Imai S, Chen D, Su F, Shiloh A, Guarente L, Gu W. Negative control of p53 by Sir2alpha promotes cell survival under stress. Cell. 2001; 107:137–148. [PubMed: 11672522]

MacDonald ML, van Eck M, Hildebrand RB, Wong BW, Bissada N, Ruddle P, Kontush A, Hussein H, Pouladi MA, Chapman MJ, et al. Despite antiatherogenic metabolic characteristics, SCD1-deficient mice have increased inflammation and atherosclerosis. Arterioscler Thromb Vasc Biol. 2009; 29:341–347. [PubMed: 19095997]

Mao B, Zhao G, Lv X, Chen HZ, Xue Z, Yang B, Liu DP, Liang CC. Sirt1 deacetylates c-Myc and promotes c-Myc/Max association. The international journal of biochemistry & cell biology. 2011; 43:1573–1581. [PubMed: 21807113]

Miyazaki M, Man WC, Ntambi JM. Targeted disruption of stearoyl-CoA desaturase1 gene in mice causes atrophy of sebaceous and meibomian glands and depletion of wax esters in the eyelid. The Journal of nutrition. 2001; 131:2260–2268. [PubMed: 11533264]

Moynihan KA, Grimm AA, Plueger MM, Bernal-Mizrachi E, Ford E, Cras-Meneur C, Permutt MA, Imai S. Increased dosage of mammalian Sir2 in pancreatic beta cells enhances glucose-stimulated insulin secretion in mice. Cell Metab. 2005; 2:105–117. [PubMed: 16098828]

Ng F, Tang BL. When is Sirt1 activity bad for dying neurons? Frontiers in cellular neuroscience. 2013; 7:186. [PubMed: 24167473]

Nin V, Chini CC, Escande C, Capellini V, Chini EN. Deleted in breast cancer 1 (DBC1) protein regulates hepatic gluconeogenesis. J Biol Chem. 2014; 289:5518–5527. [PubMed: 24415752]

Ntambi JM, Miyazaki M, Stoehr JP, Lan H, Kendziorski CM, Yandell BS, Song Y, Cohen P, Friedman JM, Attie AD. Loss of stearoyl-CoA desaturase-1 function protects mice against adiposity. Proc Natl Acad Sci U S A. 2002; 99:11482–11486. [PubMed: 12177411]

Pajvani UB, Qiang L, Kangsamaksin T, Kitajewski J, Ginsberg HN, Accili D. Inhibition of Notch uncouples Akt activation from hepatic lipid accumulation by decreasing mTorc1 stability. Nat Med. 2013; 19:1054–1060. [PubMed: 23832089]

Paton CM, Ntambi JM. Biochemical and physiological function of stearoyl-CoA desaturase. Am J Physiol Endocrinol Metab. 2009; 297:E28–E37. [PubMed: 19066317]

Paton CM, Ntambi JM. Loss of stearoyl-CoA desaturase activity leads to free cholesterol synthesis through increased Xbp-1 splicing. Am J Physiol Endocrinol Metab. 2010; 299:E1066–E1075. [PubMed: 20923962]

Pfluger PT, Herranz D, Velasco-Miguel S, Serrano M, Tschop MH. Sirt1 protects against high-fat diet-induced metabolic damage. Proc Natl Acad Sci U S A. 2008; 105:9793–9798. [PubMed: 18599449]

Qiang L, Banks AS, Accili D. Uncoupling of acetylation from phosphorylation regulates FoxO1 function independent of its subcellular localization. J Biol Chem. 2010; 285:27396–27401. [PubMed: 20519497]

Qiang L, Lin HV, Kim-Muller JY, Welch CL, Gu W, Accili D. Proatherogenic abnormalities of lipid metabolism in SirT1 transgenic mice are mediated through Creb deacetylation. Cell metabolism. 2011; 14:758–767. [PubMed: 22078933]

Qiang L, Wang L, Kon N, Zhao W, Lee S, Zhang Y, Rosenbaum M, Zhao Y, Gu W, Farmer SR, et al. Brown remodeling of white adipose tissue by SirT1-dependent deacetylation of Ppargamma. Cell. 2012; 150:620–632. [PubMed: 22863012]

Rajamohan SB, Pillai VB, Gupta M, Sundaresan NR, Birukov KG, Samant S, Hottiger MO, Gupta MP. SIRT1 promotes cell survival under stress by deacetylation-dependent deactivation of poly(ADP-ribose) polymerase 1. Mol Cell Biol. 2009; 29:4116–4129. [PubMed: 19470756]

Ramsey KM, Mills KF, Satoh A, Imai S. Age-associated loss of Sirt1-mediated enhancement of glucose-stimulated insulin secretion in beta cell-specific Sirt1-overexpressing (BESTO) mice. Aging Cell. 2008; 7:78–88. [PubMed: 18005249]

Rodgers JT, Lerin C, Haas W, Gygi SP, Spiegelman BM, Puigserver P. Nutrient control of glucose homeostasis through a complex of PGC-1alpha and SIRT1. Nature. 2005; 434:113–118. [PubMed: 15744310]

Roongta UV, Pabalan JG, Wang X, Ryseck RP, Fargnoli J, Henley BJ, Yang WP, Zhu J, Madireddi MT, Lawrence RM, et al. Cancer cell dependence on unsaturated fatty acids implicates stearoyl-CoA desaturase as a target for cancer therapy. Molecular cancer research : MCR. 2011; 9:1551–1561. [PubMed: 21954435]

Sung JY, Kim R, Kim JE, Lee J. Balance between SIRT1 and DBC1 expression is lost in breast cancer. Cancer science. 2010; 101:1738–1744. [PubMed: 20412117]

von Roemeling CA, Marlow LA, Wei JJ, Cooper SJ, Caulfield TR, Wu K, Tan WW, Tun HW, Copland JA. Stearoyl-CoA desaturase 1 is a novel molecular therapeutic target for clear cell renal cell carcinoma. Clinical cancer research : an official journal of the American Association for Cancer Research. 2013; 19:2368–2380. [PubMed: 23633458]

Wang C, Chen L, Hou X, Li Z, Kabra N, Ma Y, Nemoto S, Finkel T, Gu W, Cress WD, et al. Interactions between E2F1 and SirT1 regulate apoptotic response to DNA damage. Nat Cell Biol. 2006; 8:1025–1031. [PubMed: 16892051]

Wang YC, McPherson K, Marsh T, Gortmaker SL, Brown M. Health and economic burden of the projected obesity trends in the USA and the UK. Lancet. 2011; 378:815–825. [PubMed: 21872750]

Wong S, Weber JD. Deacetylation of the retinoblastoma tumour suppressor protein by SIRT1. Biochem J. 2007; 407:451–460. [PubMed: 17620057]

Zhao W, Kruse JP, Tang Y, Jung SY, Qin J, Gu W. Negative regulation of the deacetylase SIRT1 by DBC1. Nature. 2008; 451:587–590. [PubMed: 18235502]

Highlights

- Dbc1 ablation causes obesity and insulin resistance
- Dbc1 ablation increases Scd1 levels
- Metabolic abnormalities of *Dbc1*$^{-/-}$ are mediated by Scd1 and hepatic SirT1
- Inhibition of Scd1 decreases tumor-related death

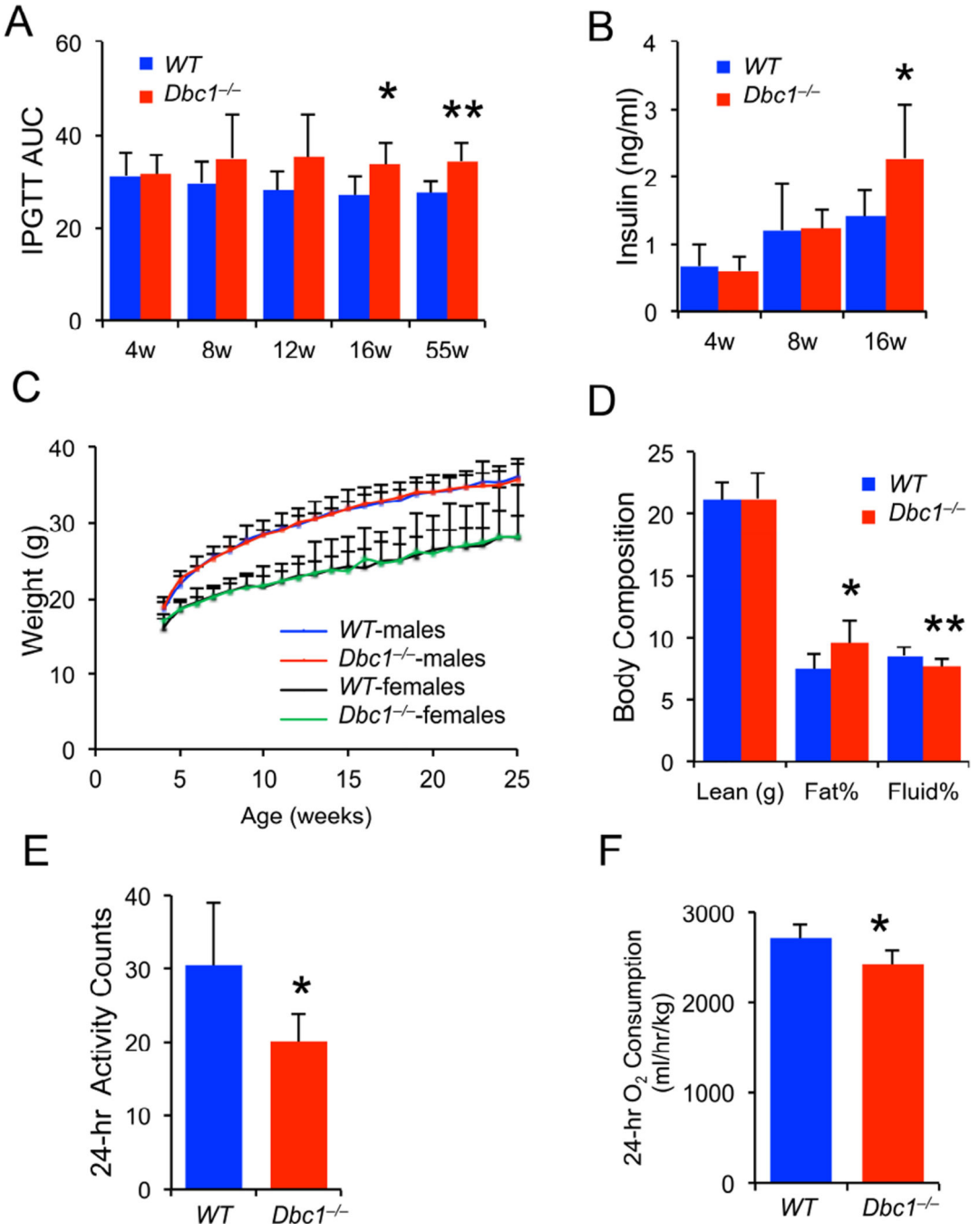

Figure 1. *Dbc1*$^{-/-}$ mice develop insulin resistance and obesity

(A) Areas under the curve (AUC) of glucose levels following intraperitoneal glucose tolerance tests (IPGTT) in chow-fed male mice of different ages (n=6 each).

(B) Plasma insulin levels of *ad libitum*-fed male mice of the indicated ages (n=9, 12).

(C) Body weight in both males and females (n=12, 9, 10, 10 each).

(D) Body composition of 8-week-old, chow-fed male mice (n=11, 8).

(E–F) Total activity counts (E) and oxygen consumption (F) in chow-fed 6-month-old male mice (n=6 each). Data represent means ± SD, * P<0.05, ** P<0.01. See also Figures S1–S3.

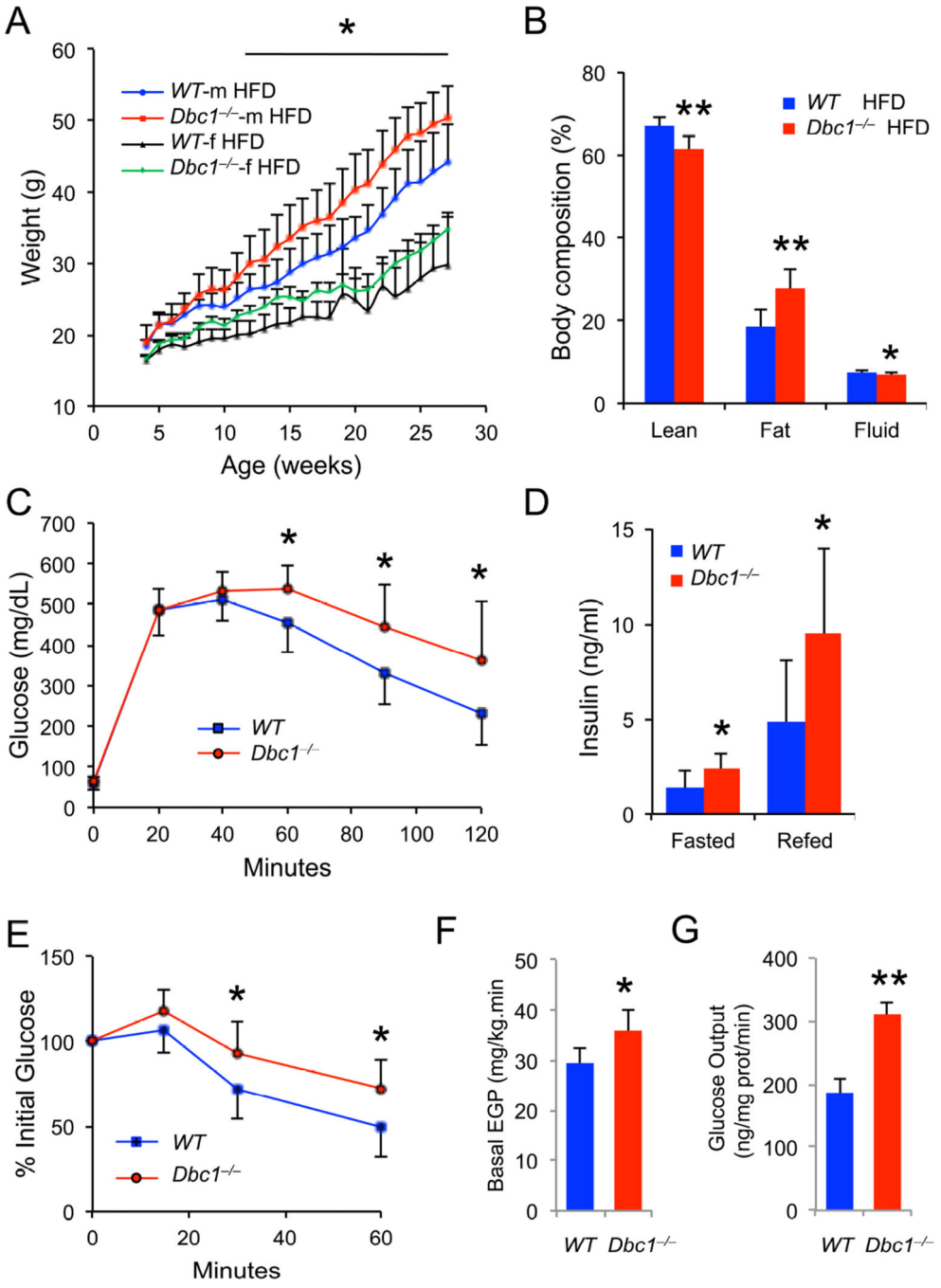

Figure 2. Metabolic abnormalities of *Dbc1*$^{-/-}$ are exacerbated by DIO

(A) Body weight of mice of both genders during high-fat diet (HFD). *P<0.05 between male wild-type and knockout mice (n=9, 9, 6, 9 respectively).

(B) Body composition following HFD for 8 weeks (n=9 each).

(C) IPGTT following HFD for 13 weeks (n=9 each).

(D) Plasma insulin levels in mice fed HFD for 24 weeks (n=7 each).

(E) ITT following 9 weeks of HFD (n=8, 10). The metabolic characterization in B–E was conducted in male mice.

(F) Basal endogenous glucose production (EGP) during hyperinsulinemic-euglycemic clamps in chow-fed male mice (n=6, 4).
(G) Glucose production in primary hepatocytes (n=3 each). Data represent means ± SD, * P<0.05, ** P<0.01.

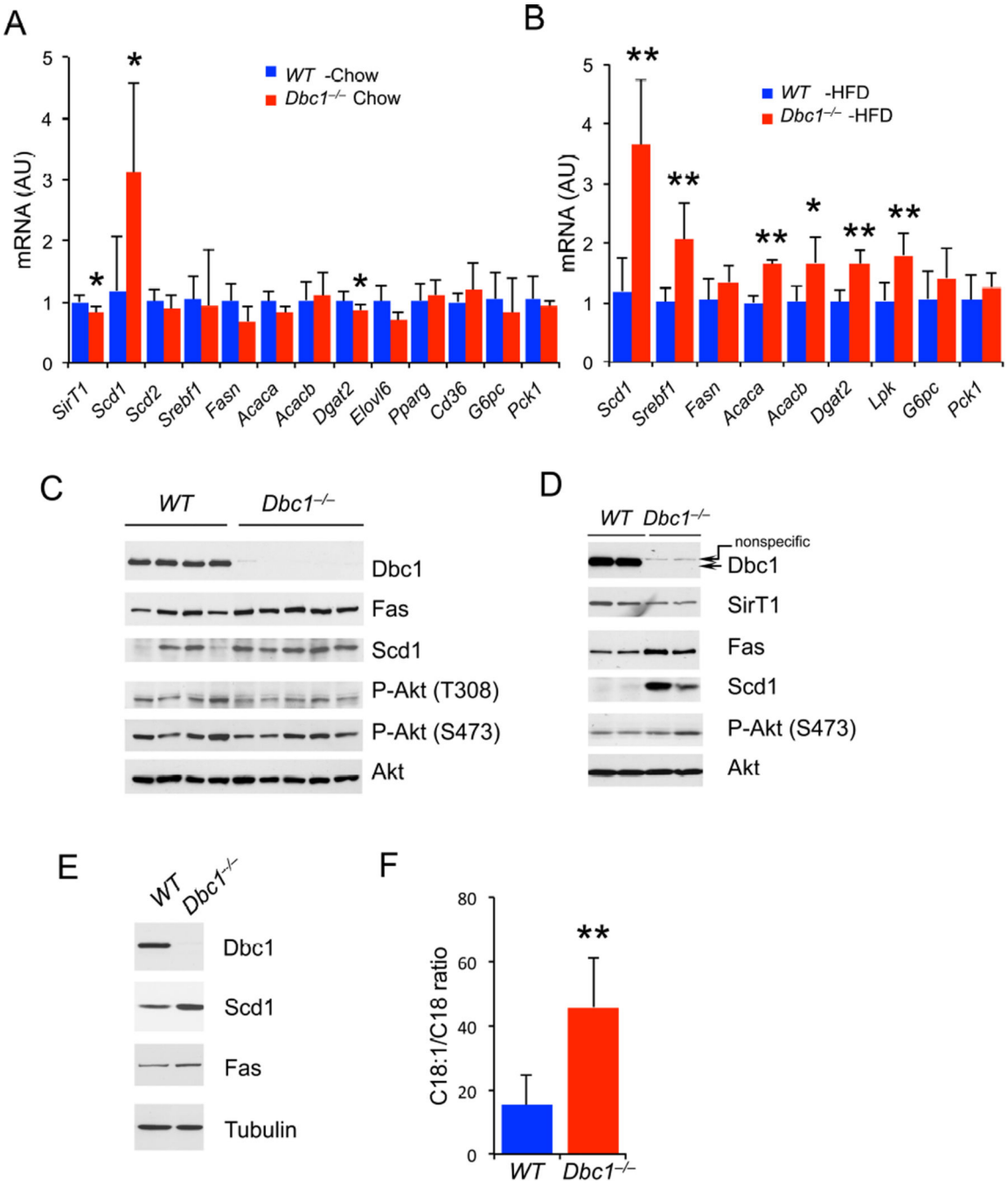

Figure 3. Increased Hepatic Scd1 in *Dbc1*$^{-/-}$ mice

(A) Q-PCR analysis of hepatic gene expression from chow-fed male mice after 4-hr re-feeding following 16-hr fasting (n=6 each).

(B) Q-PCR analysis of hepatic gene expression from male mice fed HFD for 9 weeks and fasted overnight prior to sacrifice (n=6, 7).

(C) Western blot analysis of liver protein extracts from chow-fed mice in (A).

(D) Western blot analysis of liver protein extracts from HFD-fed mice in (B).

(E–F) Western blots analysis of protein extracts (E) and Scd1 activity (F) measured by CoA levels (n=4 each) in primary hepatocytes isolated from 6-week-old mice. Data represent means ± SD, * P <0.05, ** P<0.01. See also Figure S4, Tables S1 and S2.

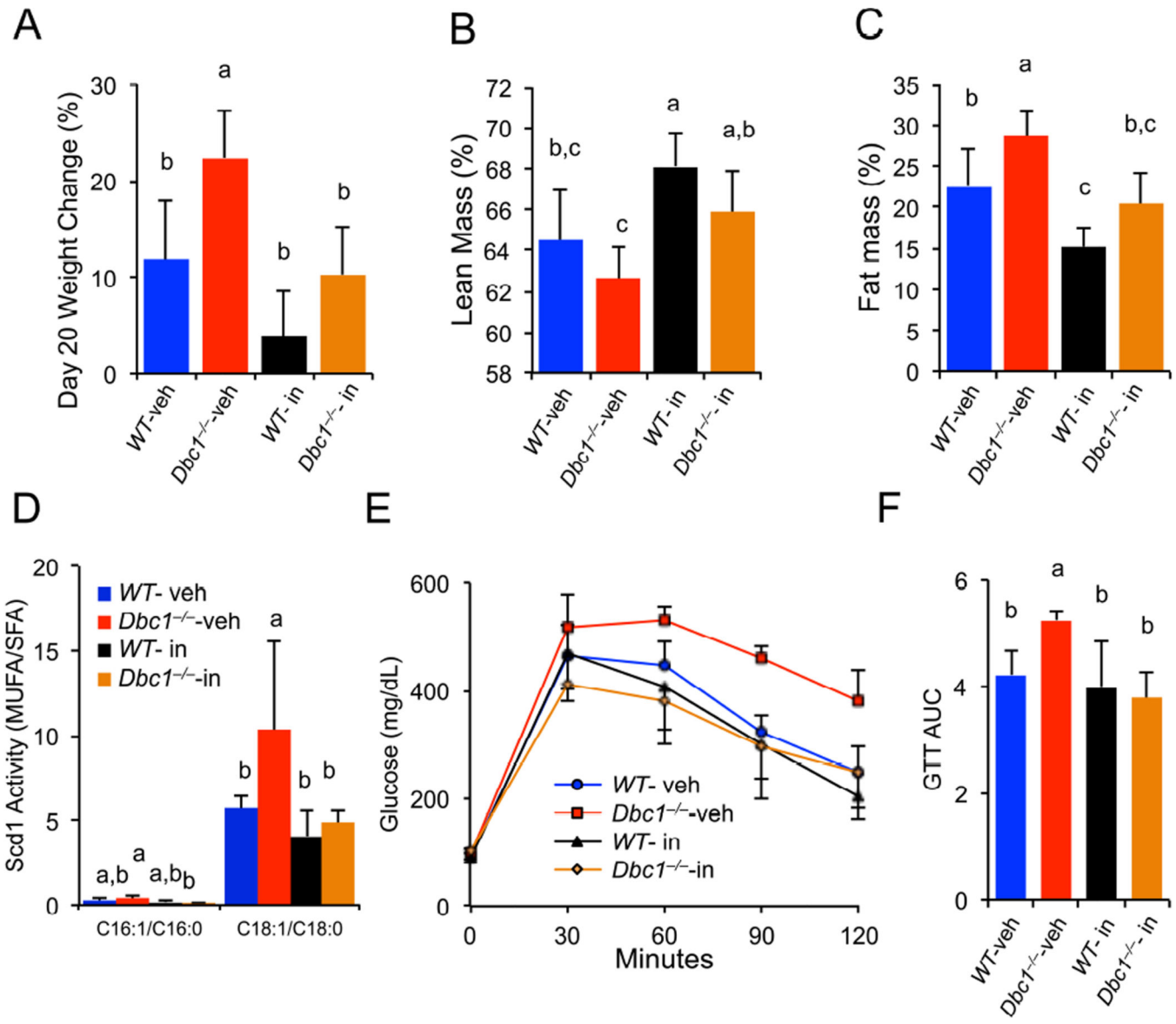

Figure 4. Inhibition of Scd1 reverses metabolic abnormalities in *Dbc1*$^{-/-}$ mice

(A) 12- to 16-week-old male mice were injected daily with Scd1 inhibitor after starting HFD-feeding. Body weight change after 20 days of treatment. P<0.0001 by two-way ANOVA.

(B) Lean mass after 18 days of treatment. P=0.001 by two-way ANOVA.

(C) Fat mass after 18 days of treatment. P<0.0001 by two-way ANOVA.

(D) Hepatic Scd1 activity plotted as MUFA to saturated FA ratios at four weeks of Scd1 inhibitor treatment. P=0.017 for C16:1/C16 and P=0.004 for C18:1/C18 by two-way ANOVA.

(E–F) IPGTT (E) and areas under curve (AUC) (F) after 3 weeks of inhibitor treatment. P=0.001 for AUC by two-way ANOVA. Statistically significant differences between two groups were calculated by post-hoc Tukey HSD test. Levels not connected by the same letter

(a, b, c) are significantly different. Data represent means ± SD, n=6 each group. See also Figure S5.

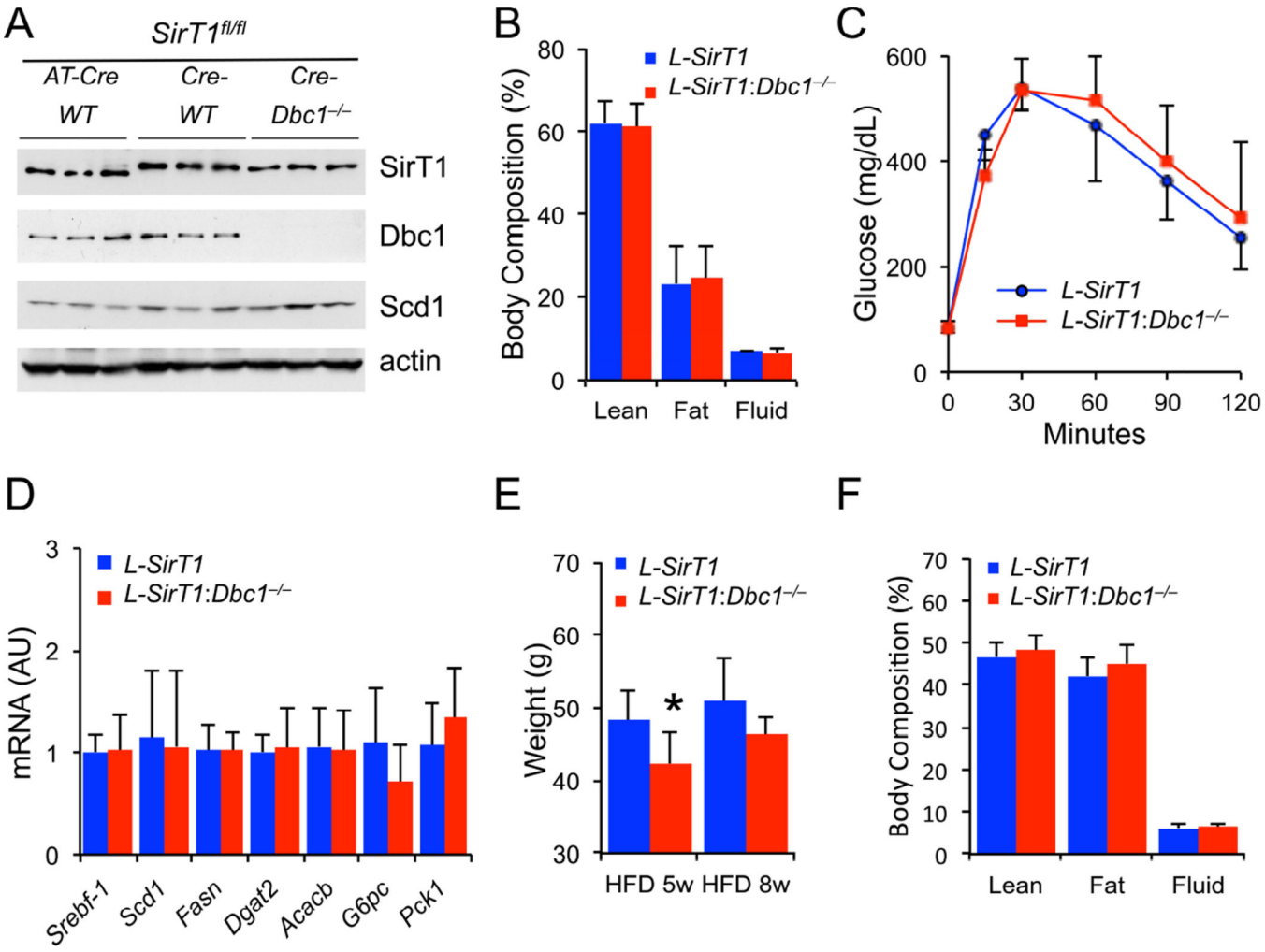

Figure 5. Metabolic abnormalities of *Dbc1*$^{-/-}$ are mediated by hepatic SirT1

(A) Validation of liver-specific SirT1 knockout (*L-SirT1*) by western blotting of liver protein extracts.

(B–C) Body composition (B) and IPGTT (C) in 19-week-old *L-SirT1* mice and double knockouts on chow diet (n=6 each).

(D) QPCR analysis of hepatic gene expression in chow-fed, overnight-fasted 21-week-old mice (n=6 each).

(E) Body weight of *L-SirT1* mice on HFD for 5 weeks or 8 weeks.

(F) Body composition after 8-week HFD (n=7, 6). All experiments were performed in male mice. Data represent means ± SD, * P<0.05. See also Figure S6.

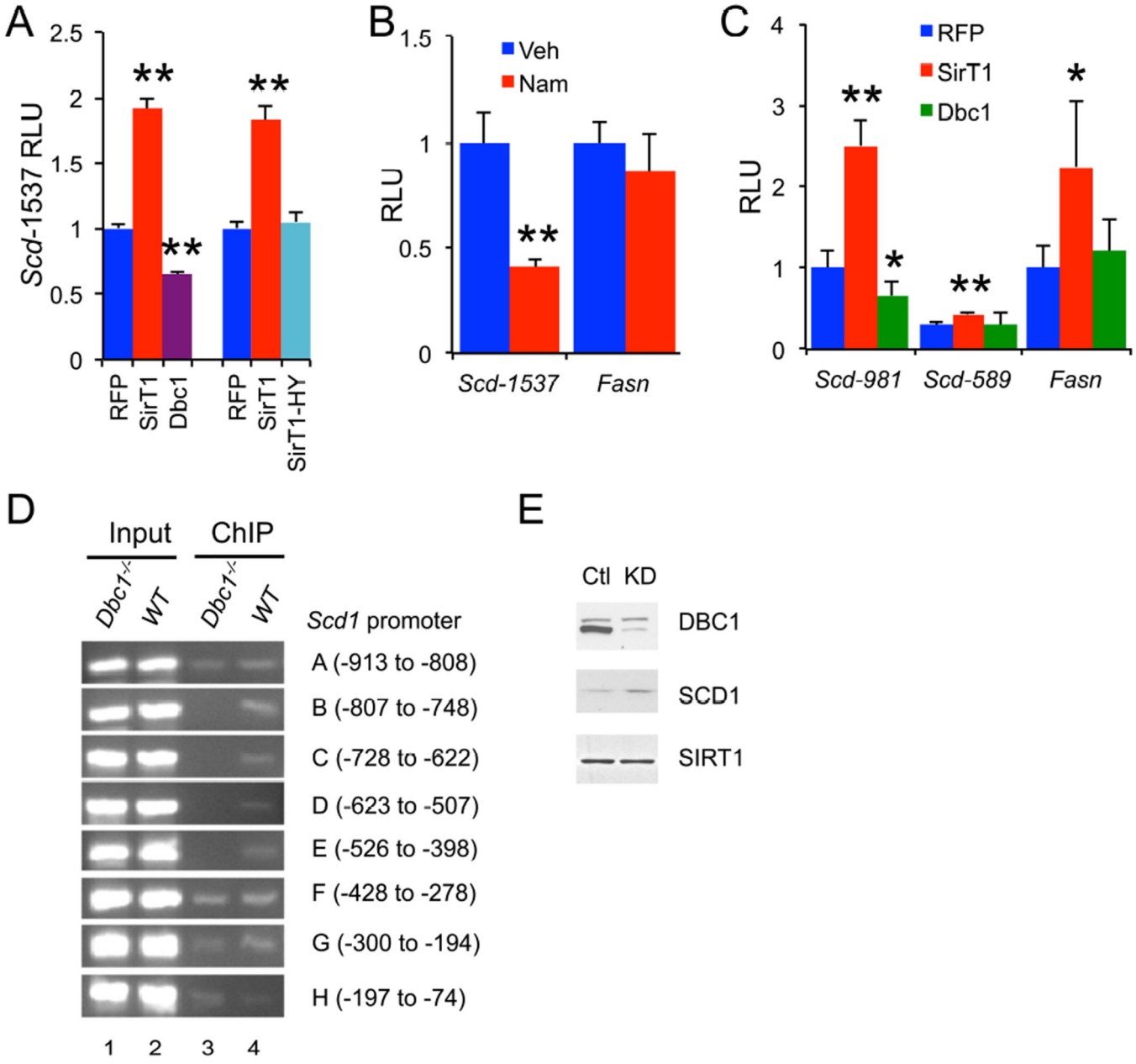

Figure 6. Dbc1 and SirT1 regulate *Scd1*

(A) *Scd1* luciferase reporter assay in 293 cells transfected with control plasmid (RFP), plasmids encoding SirT1, deacetylase-defective SirT1 mutant H363Y (HY) or Dbc1 (n=4 each).

(B) Full-length *Scd1* luciferase reporter assay in 293 cells treated with the SirT1 inhibitor 10mM nicotinamide (Nam) or vehicle (Veh) for overnight. *Fasn* reporter was used as control (n=4 each).

(C) Truncated *Scd1* promoter luciferase assay in 293 cells transfected with control plasmid (RFP), or plasmids encoding SirT1 or Dbc1. *Fasn* reporter was used as a control (n=4 each).

(D) Chromatin immunoprecipitation of Dbc1 on *Scd1* promoter in MEFs.

(E) Western blots following transient DBC1 knockdown in human lung cancer H1299 cells. Data represent means ± SD, *p<0.05, **p<0.01. Luciferase reporter assays were repeated at least three times.

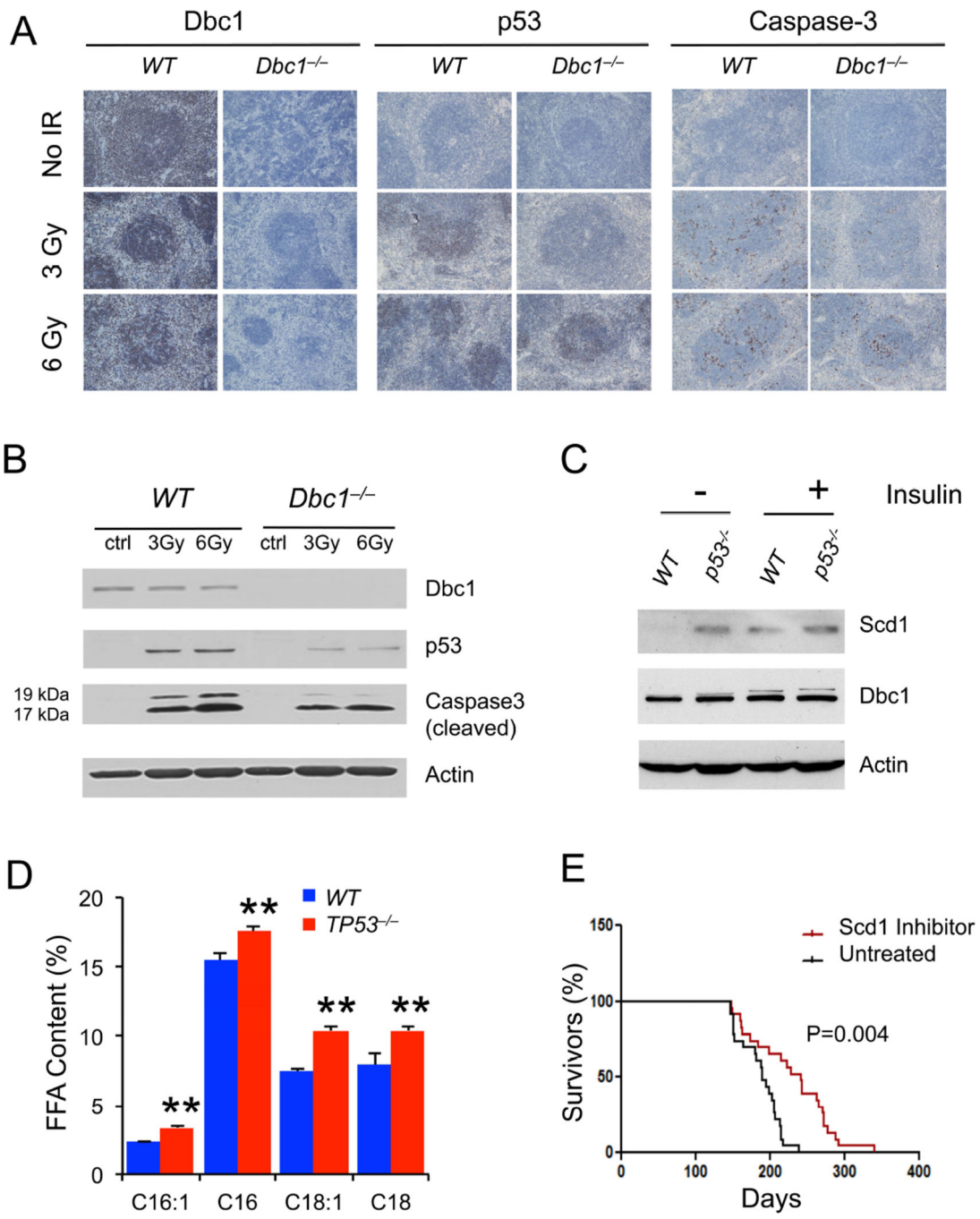

Figure 7. *Dbc1* ablation facilitates tumor progression through increased Scd1

(A) Prostate immunohistochemistry (IHC) in *Dbc1*$^{-/-}$ mice subjected to the indicated doses of γ-radiation.

(B) Western blots of spleen protein extracts from mice in (A).

(C) Western blot analysis of proteins in primary hepatocytes isolated from *TP53*$^{-/-}$ mice. Cells were treated overnight with 1.67μM insulin.

(D) MUFA content in primary hepatocytes isolated from *TP53*$^{-/-}$ mice. Data represent means ± SD, ** P<0.01 (n=4).

(E) Kaplan-Meier survival plots of *TP53*$^{-/-}$ male and female mice following treatment with Scd1 inhibitor. Statistical significance was estimated by Log-rank (Mantel-Cox) test (n=23 each). See also Figure S7.